Journal of Multidisciplinary Engineering Science and Technology (JMEST)
ISSN: 2458-9403
Vol. 6 Issue 10, October - 2019

Simulation of Increasing Positron Yield by the Interaction of Laser Wakefield Electrons with Multilayer Targets

Feng Lei, Cui Ye, Peng Meng
College of liberal arts and sciences
National University of Defense Technology
China, Changsha
feng_leii@163.com

***Abstract*—when the relativistic positrons generation is driven by ultra-intense laser, in order to increase the yield of positrons, a scheme of hitting multi-layer targets with wakefield electrons is proposed. In this scheme, the sing-layer conversion target will be replaced by the multilayer targets. The whole process of positron generation by wakefield electrons hitting on multilayer targets is simulated by Monte Carlo Program FLUKA. The results show that total positron yield under multilayer targets is about 2.4 times that of single-layer target, and the energy utilization efficiency of wakefield electrons is 1.2 times that of single-layer target. In addition, for multilayer targets, the subtarget thickness d, target spacing L and target radius R satisfy RL/d as a constant when the positron yield is maximum, when the number of target layers is more than 15, the positron yield does not increase significantly.**

Keywords—ultra-intense laser; positron yield; wakefied electrons

I. INTRODUCTION

Relativistic positron beam is an important particle beam, which is widely used in nuclear physics, particle physics and laboratory astrophysics. The MeV-level high energy positrons generated in laboratory can be used to study black holes, gamma-ray bursts, positron-electron pair plasma and positron Bose-Einstein condensation[1], while the low energy positrons (<1MeV) can be used as particle probes for nondestructive testing of materials[2]. There are three main traditional methods to generate positrons: one is using radioactive isotope β^+ decay[3]. Generally, long half-life nuclides, such as ^{22}Na, are used. The intensity of positron beam generated by this method is low. It is difficult to exceed $10^6 s^{-1}$, and the emission quality is poor. The second is based on reactor[4]. Short-lived radioisotopes, such as ^{64}Cu, are obtained by activation, and positrons are generated through β^+ decay. Thirdly, using traditional accelerators to accelerate electrons, positrons can be generated by high-energy electrons bombarding high Z target[5]. This method significantly improve positron beam intensity, but the accelerator costs are high and the floor space is large.

With the continuous development of laser technology, ultra-intense laser has been widely used in various fields, especially in the field of electron acceleration has obvious advantages[6]. Positron beams generated by ultra-intense lasers have the characteristics of high beam intensity and low cost. There are two methods to generate positrons by laser: The first is the direct method[7,8], laser irradiates solid target directly to generate hot electrons (about several MeV) on the target surface. Then these hot electrons interact with the solid target and generate positrons via the B-H process and the Trident process. The second is the indirect method[1,9, 10], laser first interacts with gas target, and generates high-energy electron (about hundreds of MeV) through laser wakefield acceleration(LWFA), then the electrons interact with solid target and generate positrons. In recent years, great development has been made in electron acceleration experiments by LWFA. The electron energy is constantly increasing, and the maximum electron energy has reached GeV. As positron yield is closely related to electron energy, the rapidly increasing electron energy makes positron generated by laser more and more attractive.

II. POSITRRON GENERATION MECHANISM

There are two processes to generate positrons in the electrons-matter interaction[11]

$$e^- + Z \rightarrow e^- + e^+ + Z \quad (1)$$

$$e^- + Z \rightarrow \gamma + e^- + Z;\ \gamma + Z \rightarrow e^- + e^+ + Z \quad (2)$$

Eq. (1) represents the Trident process. Positrons are generated directly by the interaction of electrons (> 1MeV) and target nuclei, positron yield $N_{e^+} \propto Z^2/A$. Eq. (2) represents the Beth-Heitler process. High-energy photons are produced firstly when electrons interact with nuclei in the solid target, then positrons are generated in the Coulomb field of target nuclei by pair effects, positron yield $N_{e^+} \propto (Z^2/A)^2$ [1, 12]. In order to increase positron yield, the high Z target should be selected as far as possible. The target material used in this paper is W, whose atomic number is 74, which is a good exchange for positron

generation. For thick target ($d/L_{\mathrm{rad}} > 0.01$, d is the target thickness, L_{rad} is the radiation length[12, 13], $L_{\mathrm{rad}} = 3.3$mm for W target), the B-H process plays a dominant role, and the Trident process dominates in thin target($d/L_{\mathrm{rad}} < 0.01$).

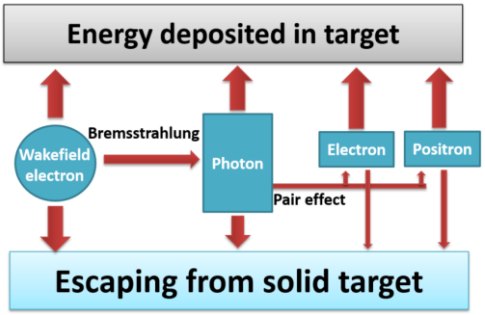

Fig.1 *Transport process of wakefield electrons in target*

Fig. 1 shows the transport process of wakefield electrons in solid target, mainly considering the bremsstrahlung of electrons and the electron pair effect of photons The energy of the wakefield electrons is eventually converted into two parts: one is the energy deposited of photons, electrons and positrons in the target; the other is the energy of photons, electrons and positrons escaping from solid target. The energy loss of wakefield electrons mainly consists of ionization and bremsstrahlung. For fast electrons, the relationship between ionization energy loss rate and bremsstrahlung energy loss rate is

$$\frac{(\mathrm{d}E/\mathrm{d}x)_{\mathrm{rad}}}{(\mathrm{d}E/\mathrm{d}x)_{\mathrm{ion}}} \approx \frac{E \cdot Z}{700} \tag{3}$$

$(\mathrm{d}E/\mathrm{d}x)_{\mathrm{rad}}$ and $(\mathrm{d}E/\mathrm{d}x)_{\mathrm{ion}}$ are bremsstrahlung energy loss rate and ionization energy loss rate respectively, and E is the energy of electrons. Because of the high energy of wakefield electrons (50～300MeV) and the high Z target, the electron energy is mainly converted to photon energy by bremsstrahlung. In addition, due to the cross section of photoelectric effect and Compton scattering is very small for high energy photons interact with the high Z target, the high energy photons are mainly converted into electron-positron pairs through electron pair effect[14].

Due to the electrons and photons escape from target, their energy can no longer be converted into the energy of positrons, witch can not be effectively utilized. In the process of positron generation, the energy utilization ratio η of wakefield electrons is defined as

$$\eta = \frac{E_{\mathrm{rad}} - E_{\gamma}}{E_{\mathrm{LWFA}}} \tag{4}$$

E_{rad} is the bremsstrahlung energy, E_{γ} is the total energy of photons escaping from solid target, E_{LWFA} is the total energy of wakefield electrons.

Both positron generation and positron annihilation occur simultaneously in solid target. On the one hand, the wakefield electrons generate positrons continuously; on the other hand, positron energy will decrease when they transporte in target, and lead to some positrons annihilate, while the other positrons escape from target. Actual positron yield can be expressed as

$$N_{\mathrm{e}^+} = N_{\mathrm{e}^+,g} - N_{\mathrm{e}^+,a} \tag{5}$$

$N_{\mathrm{e}^+,g}$ is the number of positrons generated in target and $N_{\mathrm{e}^+,a}$ is the number of positrons annihilated. When the target material and wakefield electrons are determined, the positron yield in the target is related to the thickness of the target. For Beth-Heitler process[10], $N_{\mathrm{e}^+,g} \propto d^2$. The thicker the solid target is, the higher the positron generated in target, but at the same time, the more positrons annihilate.

III. Single Target Model and Calculaion Results

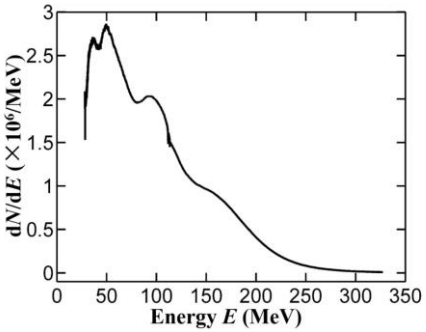

Fig.2 *Typical sperctrum of wakefield electrons*

In this paper, Monte Carlo program FLUKA[15] is used to simulate the positron generation process. All solid targets are W. The typical wakefield electron spectrum used in this paper is shown in Fig. 2. The spectra was measured by the author on 200TW laser of Shanghai Jiaotong University in June 2018. The wakefield electron number is 2.8×10^8 at one shot, the charge is 45pC, and the average energy is 97.6MeV.

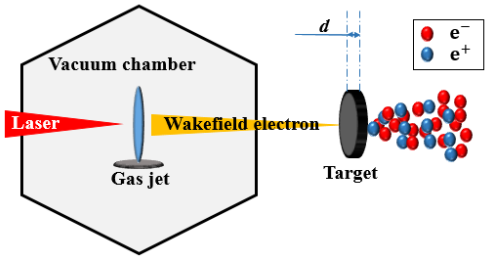

Fig.3 *Positrons generation driven by laser under single Target*

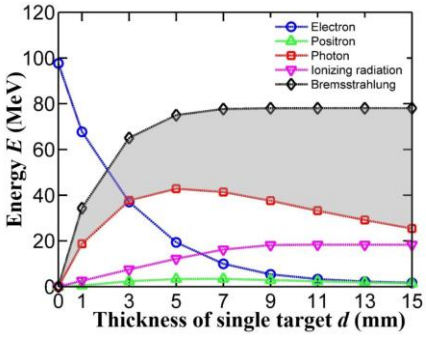

Fig.4 *The relationship between energy and target thickness of single target*

Fig. 3 shows the schematic diagram of generating positron driven by ultra-intense laser in the condition of single target. The relationship between the single target thickness and the energy of ionizing radiation, bremsstrahlung, positrons, electrons and photons behind the target is showed in Fig. 4. The shadow part is the effective utilization energy of wakefield electrons, which increases with the target thickness d. The wakefield electron energy is mainly converted to photon energy by bremsstrahlung, but the energy of photon escaping from target is also very high, which results in the waste of wakefield electron energy. The relationship between positron yield, electron energy utilization ratio and target thickness d is shown in Fig. 5. η increases with d. When d=7mm, N_{e+} reaches the highest 6.2×10^7. In this conditon, photon energy is 41.4MeV, bremsstrahlung energy is 78.2MeV, and wakefield electron energy utilization radio is 37.2%.

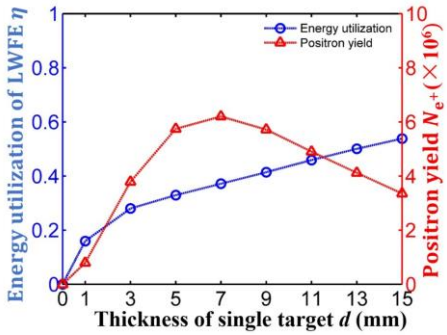

Fig.5 *The relationship between positron yield, electron energy utilization ratio and thickness of single target*

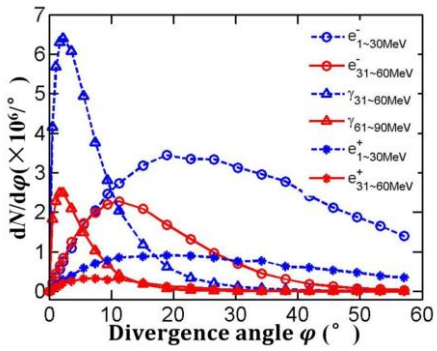

Fig.6 *Angular distribution of positrons and electrons with different energy of single target*

Fig. 6 shows the angular distribution of postions, electrons and photons in different energy groups when the wakefield electron hits a single target with thickness of 4mm, moreover, positrons, electrons and photons are obviously forward, and the higher the energy, the more obvious the forward inclination is. The divergence angle of positron is obviously larger than that of electron and photon. Fig. 7 shows the energy spectrum of positrons generated by wakefield electrons bombarding single solid target with different thickness. Low-energy positrons account for the main part, and positrons with energy of 1-30MeV account for 81-92% of the total positrons.

IV. Multilayer Target Model and Calculation Results

The schematic diagram of multilayer target structure is shown in Fig. 8. The multilayer target consists of several identical thin targets arranged orderly at fixed intervals. Among them, R is the target radius, L is the target spacing, d is the thickness of the subtarget, c is the number of target layers, $\theta = \arctan(RL/d)$.

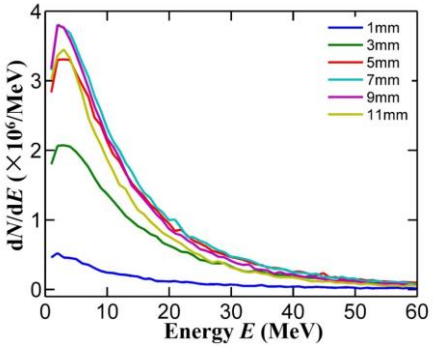

Fig.7 *Positron spectra of single target with different thickness*

For Fig. 7, low energy positrons are the main part of positrons generated by wakefield electrons. Since the divergence angle of low energy positrons is larger than that of electrons and photons, it is easier for low energy positrons to escape from multilayer target through the intervals, which effectively reduces the annihilation of positrons. As shown in Fig. 6, for electrons and photons with energy greater than 30 MeV, the divergence angle is obviously smaller than that of positrons, so they will continue to interact with the secondary target. In multilayer target, positrons, electrons and photons can be screened according to a certain divergence angle by utilizing the intervals: Only positrons with a divergence angle greater than a certain angle can escape from target through the interval, while electrons and photons with a smaller divergence angle are still trapped in the multilayer target, and continue to interact with the secondary target to generate positrons. Therefore, the multilayer target structure can effectively increase the electron energy utilization ratio and reduce the annihilation of positrons, thus increasing the positron yield.

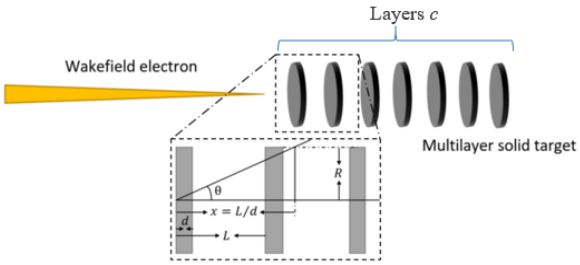

Fig.8 *Schematic diagram of multilayer targets structure*

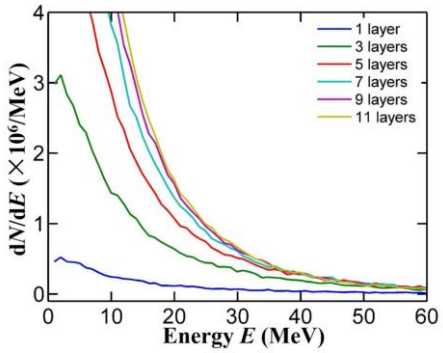

Fig.9 *Positron spectra of multilayer targets with different layers*

Fig. 9 shows the positron spectra of wakefield electrons bombarding multilayer targets with different layers. Among them, L=10mm, d=1mm, R=10mm. Compared with Fig. 7 and Fig. 9, when the positron energy is greater than 30MeV, the positron yield of multilayer target and single target is almost the same. However, when positron energy is less than 30MeV, the positron yield of multilayer targets is significantly higher than that of single target, because the multilayer target ensures that the electrons and photons are bound to the target, and the low energy positrons can escape from target, which reduces the annihilation of positrons.

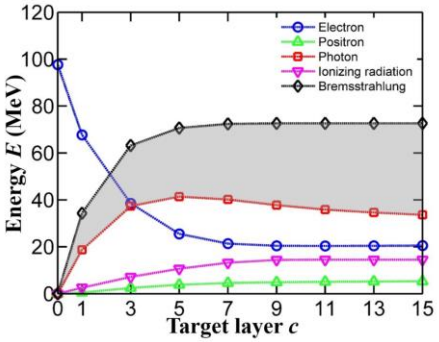

Fig.10 *The relationship between energy and layers of multilayer targets*

For the multilayer target with L=10mm, d=1mm and R=10mm, Fig. 10 shows the relationship between the energy of positrons, electrons, photons, ionizing radiation, bremsstrahlung and the number of target layers c. Fig. 11 shows the relationship between positron yield, wakefield electron energy utilization ratio and the number of target layers. From Fig. 10 and Fig. 11, when the target layers is small, wakefield electrons still have a high energy when passing through the last subtarget. Positron yield and wakefield electron energy utilization ratio both increase with the increase of the target layers. When the target layers is large, the electrons and photons passing through the last layer of target have low energy and a small amount, and the conditions for generating positrons are no longer available, the positron yield and wakefield electron energy utilization ratio do not change significantly with the increase of target layers. When the target layer number c=15, the positron yield is 1.47×108, and the wakefield electron energy utilization ratio is 44.5%, which are 2.3 times and 1.2 times corresponding to the single target respectively.

In addition, for multilayer target, from fig. 11, when d=1mm and c=15, the positron yield and the electron energy utilization rate almost reach the maximum. Keeping the total effective thickness($d \cdot c$=15mm) of multilayer target unchanged, change the thickness of subtarget d, target spacing L, target radius R, select five different target parameters, as listed in Table 1, and the relationship between positron yield and target radius is shown in Fig. 12. The maximum positron yield $N_{e^+,max}$, the multilayer target radius R_{max} corresponding to the maximum positron yield, and the ratio ξ of the multilayer target positron yield to the single target positron yield are also listed in Table 1.

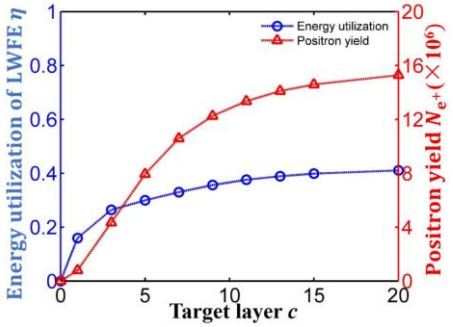

Fig.11 *The relationship between positron yield, electron energy utilization ratio and layers of multilayer targets*

From Figs. 12 and Table 1, when the positron yield of target 1, target 2 and target 3 is maximum, the target radius R_{max} remains unchanged, and the maximum positron yield increases with the decrease of subtarget thickness d. The maximum positron yield of target 1, target 4 and target 5 remains unchanged, but the target radius R_{max} increases as the target spacing L increases.

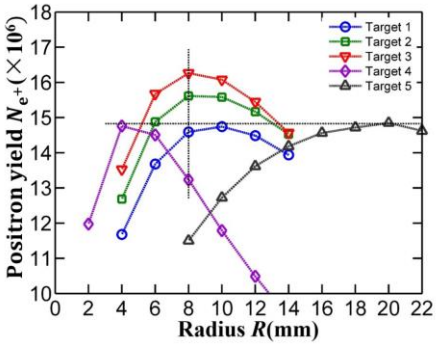

Fig.12 *The relationship between the positron yield and the radius of multilayer target*

TABLE I. CALCULATION CONDITIONS AND RESULTS OF FIVE MULTILAYER TARGETS

Target	d/mm	L/mm	$N_{e^+,max}/10^7$	R_{max}/mm	ξ
1	1	10	14.7	10	2.37
2	0.5	5	15.6	8	2.52
3	0.1	1	16.3	8	2.63
4	1	5	14.7	4	2.37
5	1	20	14.8	20	2.39

Compared with target 1, target 2 and target 3, the thicknesses of the three multilayered targets are the same under the unit axial length, that is, the total thickness of the target is 1mm per 10mm distance. In

this case, when the positron yield is the highest, the corresponding target radius $R_{\max}$ is 10, 8, 8mm, witch is almost the same, but the maximum positron yield increases gradually with the decrease of subtarget thickness. Obviously, the thin target can effectively reduce the positron annihilation in the target, but the maximum positron yield of target 3 with d=0.1mm is only 10.1% higher than that of target 1 with d=1mm, which is far less than the increase rate of multilayer target compared with that of single target. In experimental design, it is not necessary to pursue very thin subtarget, which could reduce the difficulty in making and arranging targets. Comparing target 1, target 4 and target 5, the subtarget thicknesses of the three multilayer targets are the same, d=1mm, and the target spacing L is 10mm, 5mm, 20mm, respectively. In these three cases, the maximum positron yield is almost unchanged, with $R_{\max}$ of 10mm, 4mm and 20mm, respectively. This shows that for multilayer target with subtarget thickness determined, the maximum positron yield does not change with the target spacing.

Let θ be the minimum escape angle of positrons, and define the escape coefficient ρ as

$$\rho = \tan\theta = R/x \tag{6}$$

Among them, $x = L/d \times 1\text{mm}$, so $\rho = RL/d$. For multilayer target with L=10mm, d=1mm and R=10mm, then $\theta = 45°$. It can be roughly considered that the positrons with 45°~90° divergence angle can escape from the multilayer target. The escape coefficients ρ of target 1 to target 5 in Table 1 are 1, 0.8, 0.8, 0.8 and 1, respectively. For multilayer targets, when the positron yield reaches the highest, the escape coefficients satisfies $\rho = 0.8\sim1$, that is, RL/d almost remains unchanged.

V. SUMMARY

In order to increase the positron yield, a multilayer target structure is designed when using laser wakefield electrons to bombard solid targets. By utilizing the difference of the divergence angles of positrons, electrons and photons in solid target, the particles with different energies are screened so that the lower energy positrons can escape through the interval of multilayer target, reducing the annihilation of positrons, and at the same time, the high energy electrons and photons are bound in the target to continue to interact with secondary target to generate positrons. The simulation results show that the positron yield of multilayer target is 2.4 times that of single target, and the energy utilization ratio of wakefield electrons is 1.2 times that of single target. The positron yield increases with the increase of target layers. when the number of target layers is more than 15, the positron yield no longer increases significantly. When the positron yield is the highest, the multilayer target interval L, the subtarget thickness d, and the target radius R satisfy a certain matching relationship, that is, RL/d approximately constant.

ACKNOWLEDGMENT

This work was supported by the National Natural Science Foundation of China (Grant Nos.11975308, 11690040, 11675107 and 11690043), the Science Challenge Project (Grant No. TZ2019001).

REFERENCES

[1] G. Sarri, W. Schumaker, A. Di Piazza, M. Vargas, B. Dromey, M. E. Dieckmann, et al. Table-top laser-based source of femtosecond, collimated, ultrarelativistic positron beams. Physical Review Letters, 2013, vol. 110, pp. 255002.

[2] Hautojarvi, He Yuan-jin and Yu Wei-zhong. Positron Submergence Technology. 1983.

[3] X. Guo, T. Huang. D and B Meson Decays into Vlv and PV. Chinese Physics Letters, 1991. Vol. 6, pp. 274.

[4] R. D. Han and X. Y. Zhou. Application and development of slow positron beam technology. Progress in Physics, 1999, vol. 19, pp. 305-330.

[5] T. Akahane, T. Chiba, N. Shiotani, S. Tanigawa, T. Mikado and R. Suzuki. Stretching of slow positron pulses generated with an electron linac. Applied Physics A, 1990, vol. 51, pp. 146-150.

[6] A. Pukhov, J. Meyer-Ter-Vehn. Laser wake field acceleration: the highly non-linear broken-wave regime. Applied Physics B, 2002, vol. 74, pp. 355-361.

[7] H. Chen, S. C. Wilks, D. D. Meyerhofer, J. Bonlie, C. D. Chen, S. N. Chen, et al. Relativistic Quasimonoenergetic Positron Jets from Intense Laser-Solid Interactions. Physical Review Letters, 2010, vol. 105, pp. 15003.

[8] H. Chen, S. C. Wilks, D. B. James, P. L. Edison, M. Jason, F. P. Dwight, et al. Relativistic Positron Creation Using Ultraintense Short Pulse Lasers. Physical Review Letters, 2009, vol. 102, pp. 105001.

[9] Sarri G, Poder K, Cole J M, et al. Generation of neutral and high-density electron–positron pair plasmas in the laboratory[J]. Nature Communications, 2015,6:6747.

[10] G. Sarri, W. Schumaker, A. D. Piazza, K. Poder, J. M. Cole, M. Vargas, et al. Laser-driven generation of collimated ultra-relativistic positron beams. Plasma Physics & Controlled Fusion, 2013, vol. 55, pp. 124017-124022.

[11] K. I. Nakashima and H. Takabe. Numerical study of pair creation by ultraintense lasers. Physics of Plasmas, 2002, vol. 9, pp. 1505-1512.

[12] C. Hugenschmidt, B. Löwe, J. Mayer, C. Piochacz, P. Pikart, R. Repper, et al. Unprecedented intensity of a low-energy positron beam. Nuclear Instruments & Methods in Physics Research, 2008, vol. 593, pp. 616-618.

[13] G. Berestetskii. Quantum Electrodynamics. Pergamon, Oxford: 2nd Edition, 2007.

[14] B. X. Chen, Z. Zhang. Nuclear Radiation Phusics and Explotation. Harbin Engineering University Press, 2011.

[15] G. Battistoni G. "The FLUKA code: description and benchmarking." Hadronic Shower Simulation Workshop: American Institute of Physics, 2007.